

Size dependence of lattice deformation induced by growth stress in Sn nanowires

Ho Sun Shin, Jin Yu, Jae Yong Song, and Hyun Min Park

Citation: *Appl. Phys. Lett.* **94**, 011906 (2009); doi: 10.1063/1.3064167

View online: <http://dx.doi.org/10.1063/1.3064167>

View Table of Contents: <http://apl.aip.org/resource/1/APPLAB/v94/i1>

Published by the [American Institute of Physics](#).

Related Articles

Silicon nanocrystals prepared by plasma enhanced chemical vapor deposition: Importance of parasitic oxidation for third generation photovoltaic applications

Appl. Phys. Lett. **101**, 193103 (2012)

A little ribbing: Flux starvation engineering for rippled indium tin oxide nanotree branches

Appl. Phys. Lett. **101**, 193101 (2012)

Phase constitution and interface structure of nano-sized Ag-Cu/AlN multilayers: Experiment and ab initio modeling

Appl. Phys. Lett. **101**, 181602 (2012)

Note: Axially pull-up electrochemical etching method for fabricating tungsten nanoprobe with controllable aspect ratio

Rev. Sci. Instrum. **83**, 106109 (2012)

Magnetic nanoparticles formed in glasses co-doped with iron and larger radius elements

J. Appl. Phys. **112**, 084331 (2012)

Additional information on *Appl. Phys. Lett.*

Journal Homepage: <http://apl.aip.org/>

Journal Information: http://apl.aip.org/about/about_the_journal

Top downloads: http://apl.aip.org/features/most_downloaded

Information for Authors: <http://apl.aip.org/authors>

ADVERTISEMENT



Goodfellow
metals • ceramics • polymers • composites
70,000 products
450 different materials
small quantities fast

www.goodfellowusa.com

Size dependence of lattice deformation induced by growth stress in Sn nanowires

Ho Sun Shin,¹ Jin Yu,¹ Jae Yong Song,^{2,a)} and Hyun Min Park²

¹Department of Materials Science and Engineering, Center for Electronic Packaging Materials, Korea Advanced Institute of Science and Technology, Daejeon 305-701, Republic of Korea

²Division of Advanced Technology, Korea Research Institute of Standards and Science, Daejeon 305-340, Republic of Korea

(Received 7 November 2008; accepted 14 December 2008; published online 6 January 2009)

We report on size-dependent lattice expansion of single crystalline Sn nanowires (NWs) with the wire radius (r_{NW}) = 6.9–34.7 nm, where the NWs are deposited under confinement of a nanotemplate. The longitudinal lattice expansion in the NWs increases up to approximately 1.0% with the reciprocal radius ($1/r_{\text{NW}}$), contrary to the general theoretical prediction that the surface relaxation causes lattice contraction of nanomaterials. The longitudinal dilatation of the NW lattice can be understood by the Poisson effect induced by the compressive growth stress in the radial direction, which increases with the reciprocal radius. © 2009 American Institute of Physics. [DOI: 10.1063/1.3064167]

Metallic nanowires (NWs) have attracted increasing attention for applications to nanodevices due to size effects on their functionality including variation in mechanical properties, electrical resistivity, superconductivity, thermal properties, etc.^{1–4} Size effects, which are dependent on an increase in the surface-to-volume ratio, originate from surface relaxation, which is due to imperfection of the coordination number (CN) on the metal surface.^{5,6} According to Pauli⁷ and Feibelman,⁸ the metallic radius of an atom would shrink due to reduction in the CN. Spontaneous bond contraction induces surface stress at the surface, which plays an important role in the size-dependent elasticity of NWs.^{1,9,10} According to the Bond-order-length-strength (Bond-OLS) model^{5,11–13} and atomistic computational methods,^{14–16} the lattice parameters of metallic crystals at a nanometer scale diminish with the reciprocal radius due to the surface relaxation. Many experimental studies have also demonstrated size-dependent lattice contraction.^{17–19} Therefore, the surface stress related to the surface relaxation modifies the elastic and plastic responses in nanomaterials.^{20,21} Metallic NWs shrink in the axial and radial directions with the reciprocal radius.⁵

However, to date, there have been little theoretical and experimental studies on the growth stress in metallic NWs. In this letter, we report that the crystal lattice of Sn NWs expands in the longitudinal direction depending on the wire radius and the longitudinal dilatation is ascribed to the intrinsic stress generated during the growth of the NWs.

AAO (anodic aluminum oxide) templates (8 μm thick) on aluminum substrates were prepared by a two-step anodization process at 274 K.⁴ The as-prepared templates had pore radii of $r_p = 6.9 \pm 0.5$ and 8.2 ± 0.9 nm, respectively, for the sulfuric acid electrolyte (1M, anodic voltage = 15 and 23 V, respectively) and $r_p = 13.1 \pm 2.2$ nm for the oxalic acid electrolyte (0.3M, anodic voltage = 40 V). After the pore widening process in phosphoric acid solution, the respective templates had final pore radii of $r_p = 6.9 \pm 0.5$, 8.2 ± 0.9 , 9.1 ± 1.2 , 12.4 ± 1.9 , 13.1 ± 2.2 , 18.1 ± 2.0 , 24.7 ± 1.7 , and

34.7 ± 1.5 nm, respectively. r_p was measured from twenty pores of three specimens using field emission scanning electron microscopy (Hitachi S4800). Sn NWs were electrochemically deposited onto the templates in an aqueous sulfuric electrolyte using a two-electrode system at room temperature under a sine wave voltage between 0 and -10 V. Here, because Sn cations are reduced at the cathodic potential, it is difficult for oxygen anions to be electrodeposited due to the electric field repulsion. The detailed procedure can be found in literature.⁴ As the NWs replicate the AAO pores, the pore radius (r_p) can be assumed to be equal to the NW radius (r_{NW}) in the case of small strain of less than 5% because the standard deviations of measured radii were approximately 10%. The NW length was about 4–6 μm .

In order to determine the lattice parameters of the Sn NWs, the (400) plane diffraction peaks were analyzed using x-ray diffractometry (Cu $K\alpha$ radiation, θ -2 θ scan, Bruker D8) for various wire radii, as shown in Fig. 1(a). For the calibration of diffraction angles (θ_B) of (400) plane peaks, the (400) plane diffraction peak for Si powder (NIST SRM 640c) was simultaneously measured as an internal standard ($2\theta_B = 69.132^\circ$),²² as shown in the left inset of Fig. 1(a) and plotted in the right inset. Here, several diffraction peaks were split due to diffraction by $K\alpha_2$ radiation. The Bragg diffraction angles were determined by fitting the experimental data via the pseudo-Voigt function. With the shrinkage of the NW radius in a range of $r_{\text{NW}} = 34.7$ –6.9 nm, the diffraction angles were shifted from 1 to 8, as shown in Fig. 1(a). The deformed lattice parameters (a_{NW}) in the a -axis direction of NWs were determined from the average value among the three measurements of the (400) plane diffraction angles from the Bragg condition for the tetragonal crystal structure. In this study, only the lattice constant (a_{NW}) was measured because Sn NWs have a single crystalline structure with the a -axis parallel to the pore direction of the template on which the x-ray is incident, as shown in the left inset of Fig. 1(a). Figure 1(b) shows a typical high resolution transmission electron microscopy (TEM) image and electron diffraction pattern indicating that the Sn NW had a single crystalline

^{a)}Author to whom correspondence should be addressed. Tel.: +82-42-868-5787. FAX: +82-42-868-5032. Electronic mail: jysong@kriss.re.kr.

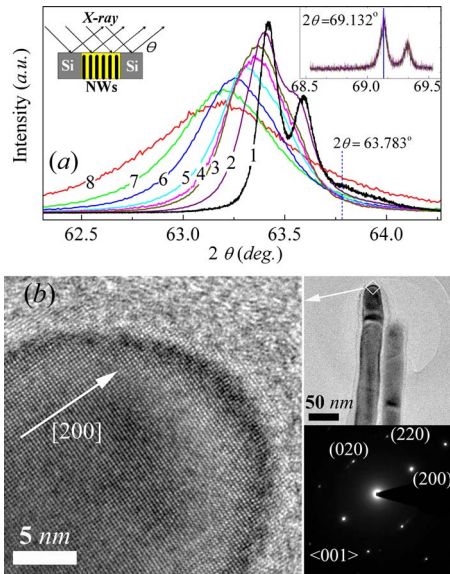


FIG. 1. (Color online) (a) X-ray diffraction patterns of (400) planes of the as-prepared Sn NWs with the wire radius (r_{NW}). Each diffraction peak is sequentially numbered from 1 to 8 for NWs with $r_{\text{NW}}=34.7\text{--}6.9\text{ nm}$. The diffraction angles (2θ) of Sn NWs are calibrated using the (400) plane peaks of the Si powder which are shown in the right inset. The left inset shows that Sn NWs are surrounded by Si powder and the x-ray beam is incident on the NWs and Si powders, simultaneously. (b) Typical high resolution TEM image and electron diffraction pattern of Sn NW ($r_{\text{NW}}=18.1\text{ nm}$) indicating a single crystalline structure in the [200] longitudinal direction.

structure oriented in the [200] longitudinal direction, in agreement with the previous results.^{3,4}

Figure 2 shows that the lattice dilatation ($\varepsilon=[a_{\text{NW}}-a_b]/a_b$) of Sn NWs for the bulk lattice parameter ($a_b=0.5831\text{ nm}$) increased with the reciprocal radius ($1/r_{\text{NW}}$) (solid circled data), reaching approximately 1.0% at $1/r_{\text{NW}}=0.15\text{ nm}^{-1}$. The question arises as to why the lattice expansion occurs in the longitudinal direction and increases with a decrease in the wire radius while the lattices of other spherical nanoclusters such as Sn, Bi, Cu, and Ni contract as the radius is reduced.^{5,12,17–19} According to the theoretical prediction of the Bond-OLS model and atomistic calculations,^{5,6,14,16} lattice contractions of nanoparticles and NWs would occur due to the effects of surface relaxation. The size-dependent contraction of the NWs can be expressed by the Bond-OLS model⁵

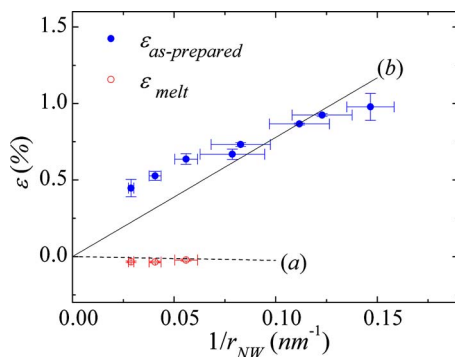


FIG. 2. (Color online) Variation in lattice deformation of Sn NWs as a function of the reciprocal radius ($1/r_{\text{NW}}$). Solid circles: as-prepared NWs ($\varepsilon_{\text{as-prepared}}$), open circles: melted NWs ($\varepsilon_{\text{melt}}$). The lattice deformation behavior with $1/r_{\text{NW}}$ is simulated by (a) Bond-OLS model [Eq. (1)] and (b) compressive growth stress model [Eq. (2)].

$$\varepsilon_{\text{BOLS}} = \sum_{i=1}^3 \frac{2D_b}{r_{\text{NW}}} \left[1 - \frac{D_b(i-0.5)}{r_{\text{NW}}} \right] c_i (c_i - 1). \quad (1)$$

Here D_b and c_i are the atomic diameters (0.372 nm) of Sn (Ref. 23) and a CN-determined bond contraction factor of atoms at the i th layer from the surface, respectively. In a previous report, c_1 was deduced as 0.9966 via a Bond-OLS simulation of experimental results where the a -axis lattice parameter of Sn nanoparticles contracted up to 0.07% at $r=4.6\text{ nm}$.¹¹ Here, it is assumed that $c_i=1$ for $i>1$ for simplicity. As shown in Fig. 2(a), the longitudinal lattice contraction increases slowly with the reciprocal radius according to Eq. (1).

Thus, the lattice expansion observed in the present study is opposite to the effects of surface relaxation inducing lattice contraction of nanostructures. Recently, it was reported that Si NWs can be expanded when they are passivated by hydrogen.²⁴ Also, although an expansion of the lattice constant in Pd nanocrystals was observed, it was due to pseudomorphism in the case of crystalline supports or the incorporation of impurities into the Pd lattice.^{17,25} In this study, the amorphous character of an AAO nanotemplate leads to negligible pseudomorphism. After melting the Sn NWs ($r_{\text{NW}}=18.1, 24.7, 34.7\text{ nm}$) in templates at $400\text{ }^\circ\text{C}$ and solidifying them under vacuum (10^{-3} Torr), the lattice strains ($\varepsilon_{\text{melt}}$) were relaxed to approximately zero, as shown in Fig. 2 (open circled data). The relaxation of elastic strain after melting excludes the incorporation effects of impurities such as O_2 and H_2 . If any, the incorporation effects would be sustained despite the thermal treatment. Also, the melting temperature depressions of Sn NWs with the reciprocal radius in the previous study exclude the oxygen incorporation, which is known to increase the melting temperature according to the Sn–O binary phase diagram.²⁶

The longitudinal lattice expansions can be understood by the following mechanism: an external compressive stress is exerted on the wire in the radial direction and the lattice expands due to the Poisson effect. The compressive stress is termed *growth stress* evolving in the NWs when they are electrochemically deposited under confinement of a template. Although the origin of the growth stress in the NWs is not clear at the moment, it should be constant regardless of the wire radius when the electrodeposition conditions, such as growth rate, temperature, and pH, are same. The growth stress in the NW is comparable to the stress force (N/m) evolving during thin film growth on a substrate, an intrinsic property which is invariable for the same film deposition process.^{27,28} In this study, however, the growth stress-induced strain increases with the reciprocal radius. This suggests that the NW growth stress is a function of the wire radius. For an external surface stress force ($\eta, \text{N/m}$) exerted on a unit surface length of the sphere with a radius (r), the inward pressure exerted on the sphere is expressed as $2\eta/r$ according to the Laplace–Young relation. The factor of 2 originates from the spherical shape. Similarly, for a cylindrical NW, the compressive growth stress (σ_G) can be deduced as $\sigma_G=\eta/r_{\text{NW}}$. Figure 3 depicts that an intrinsic growth stress σ_G is externally applied to the cylindrical NW with open ends under a plane stress condition ($\sigma_{zz}=0$). The Lamé formula yields $\sigma_{rr}=\sigma_{\theta\theta}=-\sigma_G$ when only external pressure is applied to a cylindrical NW.²⁹ The boundary conditions are $\sigma_{rr}=-\sigma_G$ at $r=r_{\text{NW}}$ and the displacement is zero at $r=0$,

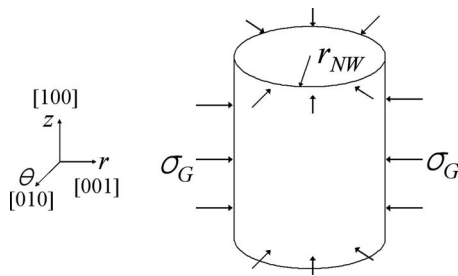


FIG. 3. A schematic of a cylindrical NW in a state of compressive growth stress (σ_G) under a plane stress condition with open ends.

respectively. According to Hooke's law, the longitudinal strain due to the growth stress can be written as

$$\varepsilon_G = 2\nu\eta/E_b r_{NW}, \quad (2)$$

and the corresponding lattice contraction is derived as $\varepsilon_{rr} = -(1-\nu)\sigma_G/E_b$.²⁹ Optimized curve fitting of the experimental data via Eq. (2) yields $\eta=8.7$ N/m, as shown in Fig. 2(b). Here, $\nu=0.34$ and $E_b=76$ GPa are used³⁰ and the lattice contractions due to the surface relaxation [according to Eq. (1)] are neglected as they are very small in comparison with the lattice expansion due to the growth stress. Interestingly, when $\eta=8.7$ N/m, Eq. (2) describes well the size-dependent lattice expansion of Sn NWs in a range of $1/r_{NW}=0.03-0.15$ nm⁻¹ despite some deviations. This implies that a compressive growth stress of 870 MPa is exerted on a NW with $r_{NW}=10$ nm, for example. It is noted that the size dependency of the elastic modulus needs to be incorporated into Eq. (2) because the elastic modulus is also size dependent in the nanometer scale^{1,5,13} and will be considered in future work.

In summary, a size-dependent longitudinal lattice expansion of Sn NWs was observed. This is ascribed to the Poisson effect due to the compressive growth stress exerted in the radial direction of the NW. Growth stress is intrinsically generated during electrodeposition and increases with the reciprocal radius. Further studies on the physical origin of the growth stress during template-supported deposition are needed because the residual stress can influence the

electrical and mechanical properties of one-dimensional nanomaterials.

This work was supported by the Center for Electronic Packaging Materials (ERC) of MEST/KOSEF.

- ¹G. Y. Jing, H. L. Duan, X. M. Sun, Z. S. Zhang, J. Xu, Y. D. Li, J. X. Wang, and D. P. Yu, *Phys. Rev. B* **73**, 235409 (2006).
- ²Q. Huang, C. M. Lilley, M. Bode, and R. Divan, *J. Appl. Phys.* **104**, 023709 (2008).
- ³M. Tian, J. Wang, J. Snyder, J. Kurtz, Y. Liu, P. Schiffer, T. E. Mallouk, and M. H. W. Chan, *Appl. Phys. Lett.* **83**, 1620 (2003).
- ⁴H. S. Shin, J. Yu, and J. Y. Song, *Appl. Phys. Lett.* **91**, 173106 (2007).
- ⁵C. Q. Sun, *Prog. Solid State Chem.* **35**, 1 (2007), and references therein.
- ⁶W. J. Huang, R. Sun, J. Tao, L. D. Menard, R. G. Nuzzo, and J. M. Zuo, *Nature (London)* **7**, 308 (2008).
- ⁷L. Pauling, *J. Am. Chem. Soc.* **69**, 542 (1947).
- ⁸P. J. Feibelman, *Phys. Rev. B* **53**, 13740 (1996).
- ⁹H. Liang and M. Upmanyu, *Phys. Rev. B* **71**, 241403 (2005).
- ¹⁰S. Cuenot, C. Frétiigny, S. Demoustier-Champagne, and B. Nysten, *Phys. Rev. B* **69**, 165410 (2004).
- ¹¹C. Q. Sun, *J. Phys.: Condens. Matter* **11**, 4801 (1999).
- ¹²G. Apai, J. F. Hamilton, J. Stohr, and A. Thompson, *Phys. Rev. Lett.* **43**, 165 (1979).
- ¹³C. Q. Chen, Y. Shi, Y. S. Zhang, J. Zhu, and Y. J. Yan, *Phys. Rev. Lett.* **96**, 075505 (2006).
- ¹⁴H. S. Park and P. A. Klein, *Phys. Rev. B* **75**, 085408 (2007).
- ¹⁵S. K. Kwon, Z. Nabi, K. Kádas, L. Vitos, J. Kollár, B. Johansson, and R. Ahuja, *Phys. Rev. B* **72**, 235423 (2005).
- ¹⁶Y. Wen, Y. Zhang, and Z. Zhu, *Phys. Rev. B* **76**, 125423 (2007).
- ¹⁷R. Lamber, S. Wetjen, and N. I. Jaeger, *Phys. Rev. B* **51**, 10968 (1995).
- ¹⁸Q. Jiang, L. H. Liang, and D. S. Zhao, *J. Phys. Chem. B* **105**, 6275 (2001).
- ¹⁹A. M. Stoneham, *J. Phys.: Condens. Matter* **11**, 8351 (1999).
- ²⁰M. R. Shankar and A. H. King, *Appl. Phys. Lett.* **90**, 141907 (2007).
- ²¹E. W. Wong, P. E. Sheehan, and C. M. Lieber, *Science* **277**, 1971 (1997).
- ²²Joint Committee Powder Diffraction Standards (JCPDS) International center for diffraction data, PDF No. 27-1402, Swarthmore, PA, 2003.
- ²³K. K. Nanda, S. N. Sahu, and S. N. Behera, *Phys. Rev. A* **66**, 013208 (2002).
- ²⁴B. Lee and R. E. Rudd, *Phys. Rev. B* **75**, 041305 (2007).
- ²⁵J. W. Jacobs and D. S. Schryvers, *J. Catal.* **103**, 436 (1987).
- ²⁶S. Cahen, N. David, J. M. Fiorani, A. Maitre, and M. Vilasi, *Thermochim. Acta* **403**, 275 (2003).
- ²⁷R. C. Cammarata, *Prog. Surf. Sci.* **46**, 1 (1994).
- ²⁸A. L. Shull and F. Spaepen, *J. Appl. Phys.* **80**, 6243 (1996).
- ²⁹A. C. Ugural and S. K. Fenster, *Advanced Strength and Applied Elasticity*, 3rd ed. (Prentice-Hall, Englewood Cliffs, NJ, 1995).
- ³⁰R. Ravelo and M. Baskes, *Phys. Rev. Lett.* **79**, 2482 (1997).